# The *AGILE* Cycle-1 Coverage and Exposure. How We Detect Galactic Sources.

S. VERCELLONE[1], S. SOLDI[1,2], A. CHEN[1,3], A. GIULIANI[1,3], S. MEREGHETTI[1], A. PELLIZZONI[1], M. TAVANI[4]
[1] *IASF-CNR, Sezione di Milano, Milano, Italy*
[2] *Univesità degli Studi di Milano, Dipartimento di Fisica, Milano, Italy*
[3] *Consorzio Interuniversitario Fisica Spaziale, Torino, Italy*
[4] *IASF-CNR, Sede di Roma, Roma, Italy*

**ABSTRACT.** We made use of a possibile *AGILE* Cycle-1 Pointing Program to study Galactic *EGRET* unidentified sources and $\gamma$-ray pulsars. We compare our simulated results with the *EGRET* data and draw conclusions upon the *AGILE* capabilities in observing galactic sources.

## 1. Introduction

One of the most puzzling results of the *EGRET/CGRO* mission is that approximately 60% (171 sources) of the $\gamma$-ray sources listed in the $3^{rd}$ *EGRET* Catalog lack a plausible identification (Hartman et al., 1999). About 70 of those sources lie along the Galactic Plane ($|b| \leq 10°$), where we expect to see $\gamma$-ray pulsars, whose observed number is less than 10% of the possible targets.

Solving the mystery of $\gamma$-ray unidentified sources and discovering new $\gamma$-ray pulsars are two key projects of the *AGILE* Mission (Tavani et al., 1999), sensitive in the hard X-ray (10-40 keV) and $\gamma$-ray (30 MeV-50 GeV) energy bands, planned to be operational during the years 2005-2008.

## 2. The Galactic Center coverage during the *AGILE* Cycle-1

*AGILE* (Tavani et al., 2004 and references therein) is an ASI mission to be launched in the second half of 2005. For the first time in $\gamma$-ray space missions, *AGILE* will have on board a Silicon strip detector for $\gamma$-ray imaging in the energy band 30 MeV - 50 GeV (the Gamma-Ray Imaging Detector, *GRID*), and a hard X-ray monitor (Super-AGILE, *SA*), sensitive in the 10 - 40 keV energy band. *AGILE* performance will allow a significant improvement in detection capability and source location accuracy compared to *EGRET*. The nearly constant sensitivity across the wide ($\sim$ 3sr) field of view (FOV) will allow the detection of $\gamma$-ray transient events occuring not only near the instrument axis, but also at large ($\sim 60°$) off-axis angle. The simultaneous monitoring of sources in the hard X-ray band will allow on-board multiwavelength studies of a subclass of "co-operative" objects, flaring simultaneously in the two bands within a radius of $\sim 30°$ from the pointing direction. The *AGILE* spacecraft imposes some constraints on the pointing strategy. Due to the solar panel constraints, the majority of sources will drift within the *AGILE* FOV by $\leq 1°$/day, making the off-axis performance extremely important for our instrument. A possible *AGILE* pointing strategy could envision two different periods: 1) during the first year (Cycle-1) the whole sky would be covered by means of 6 pointings lasting 60 days each. Fig. 1 shows the GRID FOVs at the beginning of each pointing, superimposed on the occultation factor due to the Earth transits within the GRID FOV; 2) the second year of operations (Cycle-2) could be devoted to deep observations of the Galactic Center (GC) and of the regions near the Celestial Poles, where the occultation factor is minimum. A preliminary strategy could foresee about 6 months of observation on the GC, 3 months pointing towards the North Celestial pole, and another 3 months pointing towards the South Celestial pole.

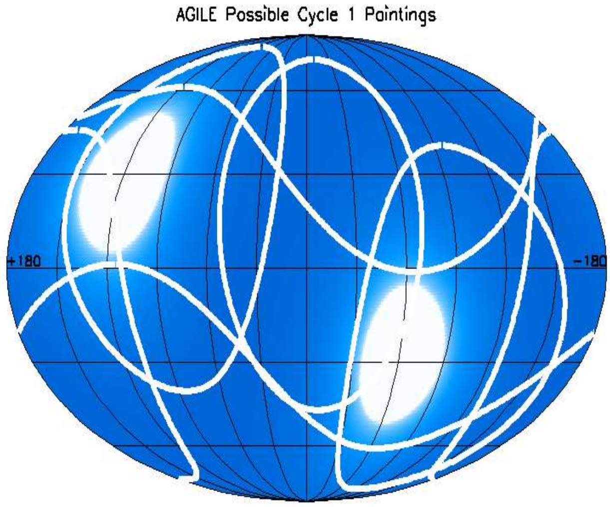


Fig. 1. A possible *AGILE* pointing strategy (*AGILE* Cycle-1). White circles are the initial positions of the *AGILE*-GRID FOV for the six pointings. The gray-scale background represents the Earth occultation factor (for a detailed discussion on the *AGILE* exposure see Pellizzoni et al., 2001); brighter areas correspond to unocculted sky regions near the Celestial Poles. The maximum occultation factor (occuring along the Ecliptic) is about 40%.

TABLE I

Parameters for the simulated pointings towards the galactic center and 2CG 135+1. We report the viewing period number (VP), the Galactic longitude and the Galactic latitude for each pointing. Each pointing lasts about 1 week.

| VP | Gal. longitude | Gal. latitude | VP | Gal. longitude | Gal. latitude |
|---|---|---|---|---|---|
| | *Galactic Center* | | | *2CG 135+1* | |
| 1.09 | 349.53 | 26.85 | 3.27 | 93.27 | 18.15 |
| 1.10 | 353.15 | 21.78 | 3.28 | 94.64 | 18.93 |
| 2.11 | 351.25 | 13.47 | 3.29 | 95.84 | 19.82 |
| 2.12 | 354.47 | 8.40 | 3.30 | 96.85 | 20.82 |
| 2.13 | 357.55 | 3.29 | 4.38 | 163.45 | -34.22 |
| 2.14 | 0.53 | -1.86 | 4.39 | 167.43 | -29.55 |
| 2.15 | 2.59 | -7.50 | 4.40 | 171.06 | -24.75 |
| 2.16 | 5.50 | -12.64 | 5.41 | 170.22 | -15.02 |
| 2.17 | 8.46 | -17.77 | 5.42 | 173.39 | -10.14 |
| 2.18 | 10.56 | -23.36 | 5.43 | 173.39 | -10.14 |

### 2.1. Galactic Center and 2CG 135+1 simulations

In Table I we report the pointing scheme of the two simulated fields, the Galactic Center and the variable unidentified galactic source 2CG 135+1. These simulations have been performed in order to: 1) test the *AGILE* Likelihood code performance (*ALIKE*, Chen 2004) in automatically detecting multiple sources (the Galactic Center); 2) test the *AGILE* performance in detecting mid-intensity sources ($F_{E>100MeV} \leq 70 \times 10^{-8}$ ph cm$^{-2}$ s$^{-1}$) along the Galactic plane (2CG 135+1).

Fig. 2 shows the *AGILE* pointings, as obtained following the *AGILE* Cycle-1 scheme, for the Galactic Center Region (left panel) and towards 2CG 135+1 (right panel). In

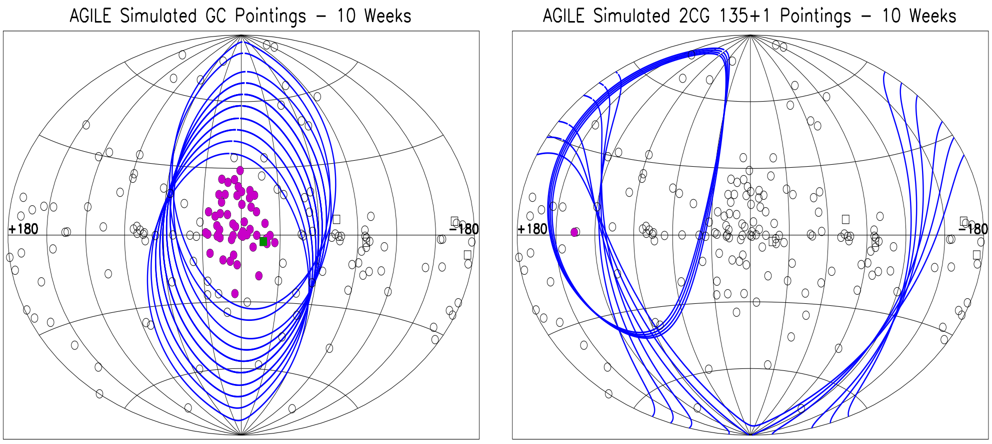


Fig. 2. *Left Panel:* AGILE Cycle-1 pointings towards the Galactic Center. Filled circles represent EGRET unidentified sources, filled squares are gamma-ray pulsars. Open symbols represent sources outside the Galactic Center region ($|l|$ , $|b| \geq 30°$ ). Circular lines represent the AGILE field of view during the 10 week pointings. Each line represents a one-week pointing. *Right Panel:* AGILE Cycle-1 pointings towards the Galactic source 2CG 135+1. Open symbols represent gamma-ray pulsars (squares) and unidentified sources (circles). The filled circle marks the position of 2CG 135+1.

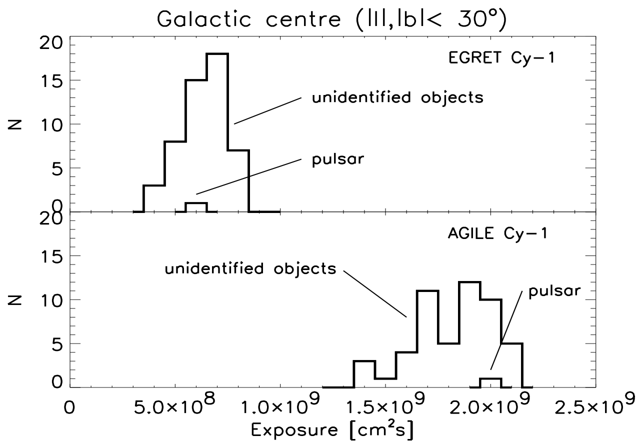


Fig. 3. Exposure distribution for the Galactic Center sources ($|l|$ , $|b| \leq 30°$ ) for *EGRET* (upper panel) and *AGILE* (lower panel) at the completion of their Cycle-1 programs.

both panels, the sources represented by filled circles are those under investigation.

Fig. 3 shows the exposure distribution for the sources near the Galactic Center at the completion of *EGRET* and *AGILE* Cycle-1, while Fig. 4 shows the stacked counts map, centered in the Galactic Center, obtained after the 10-week observation of Table I. At the completion of the first year of observation, *AGILE* will accumulate an exposure on the Galactic Center region a factor of 2-3 greater than that of *EGRET* . This will allow detailed variability studies of unidentified sources populating this region by mean of a continous sequence of pointings.

The *AGILE* simulated sky for the 10-week observation of Table I towards the Galactic

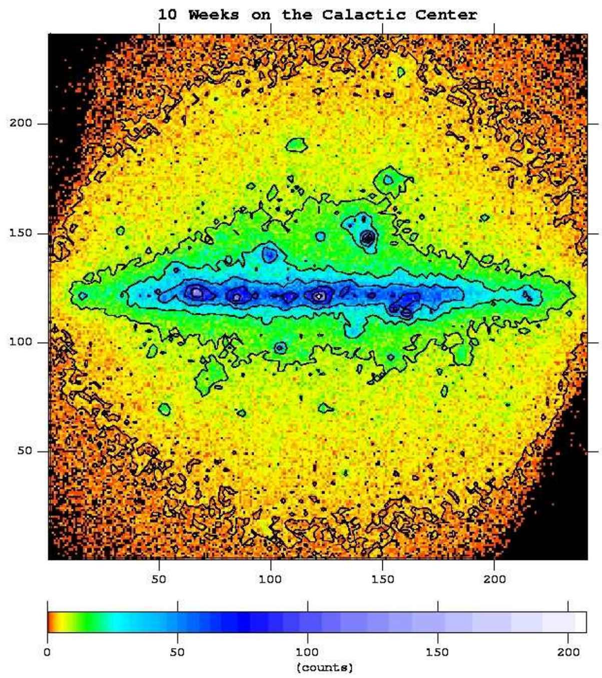


Fig. 4. Stacked counts map, centered in the Galactic Center, obtained by summing up 10 observations lasting 1 week each.

Center is representative of the $\gamma$-ray sources falling within the *AGILE* FOV, the Galactic and isotropic $\gamma$-ray background and the residual particle background (assumed to be 0.1 Hz). The diagonal shape of the image is due to the changes of the pointing directions according to Table I.

The Galactic source 2GC 135+1 is a very good candidate for testing the source location and source separation perfomance of $\gamma$-ray instruments. This source (2GC 135+1 $\equiv$ 3EG J0241+6103) is located on the Galactic plane and is probably associated with the variable radio source GT 0236 + 610 (Gregory et al., 1979, Tavani et al., 1996). Fig 5 shows the *ALIKE* results for the *AGILE* simulation of Table I pointings towards 2GC 135+1, performed stacking 10 pointings lasting $\sim$ 1 week each, selected from the Cycle-1 pointing scheme, in order to keep the source $> 37°$ away from the GRID axis. The results of this simulation confirms the *AGILE* capability of separating close ($\Delta \simeq 1.5°$), weak ($F_{\rm E>100MeV} \sim 40-70\times10^{-8}\,{\rm ph\,cm^{-2}s^{-1}}$) sources also at high off-axis angles ($\theta > 30°$).

## 3. All-sky survey: *AGILE* vs. *EGRET*

*EGRET* performed an all-sky survey during its 18-month Cycle-1 by means of more than 50 different pointings lasting, on average, two weeks each. The *EGRET* FOV was about 0.8 sr and the sensitivity across it was not uniform, because of a sharp cut-off in the effective area, namely, $A_{\rm eff}[20°] \approx 0.5 \times A_{\rm eff}[0°]$, and $A_{\rm eff}[40°] \approx 0.04 \times A_{\rm eff}[0°]$ at $E = 100$ MeV. For this reason, *EGRET* was able to efficiently detect and monitor sources only at small off-axis angles, marginally exploiting the overlaps of different pointings.

*AGILE* suffers only a moderate loss of sensitivity across its wide ($\sim 3\,$sr) FOV, thanks to gently decreasing effective area for off-axis angles: the effective area halves at an off-

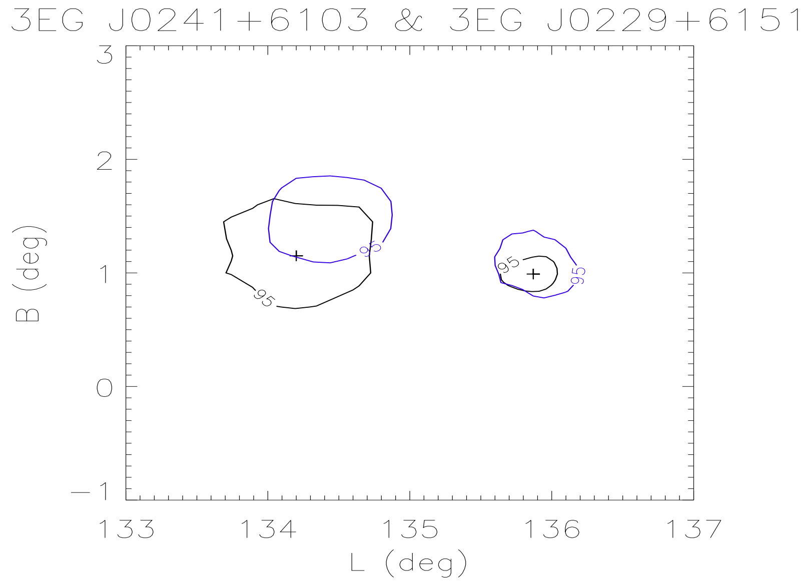


Fig. 5. Likelihood 95% confidence contours for the Galactic Plane sources 3EG J0241+6103 (2GC 135+1) and the nearby 3EG J0229+6151. Blue and black contours are the *AGILE* and the *EGRET* ones, respectively.

axis angle of $\sim 60°$. If we take into account the ratio $R = A_{\rm eff}^{\rm AGILE}/A_{\rm eff}^{\rm EGRET}$ as a function of the off-axis angle $\theta$ we obtain the following values: $R \sim [0.5, 0.7, 1.0, 2.3, 9.8, \infty, \infty]$ for off-axis angles $\theta = [0, 10, 20, 30, 40, 50, 60]$. This result shows that, above 20°, the *AGILE* effective area is always greater than that of *EGRET* , increasing the chance of detecting transient sources and allowing long-term monitoring of candidate and confirmed $\gamma$-ray sources.

Fig. 6 (left panel) shows the *EGRET* exposure distribution for different classes of $\gamma$-ray sources, accumulated during the first year and half of *EGRET* observations (Apr. $22^{nd}$ 1991 - Nov. $17^{th}$ 1992). The right panel shows the *AGILE* Cycle-1 exposure distribution for the same sources. We considered the first year of observation, simplifying the pointing program into 6 major viewing periods, each divided into 10 sub-periods of approximately 1 week each.

A remarkable difference is present in the shape of the exposure distribution of the unidentified sources; while for *EGRET* the majority of them have accumulated an exposure *lower* than $\sim 1 \times 10^9$ cm$^2$s, and the peak of the exposure distributions for *EGRET* is at $\sim 0.6 \times 10^9$ cm$^2$s, for *AGILE* all but few have exposure *greater* than $\sim 1 \times 10^9$ cm$^2$s and the peak of the exposure distribution is at $\sim 2 \times 10^9$ cm$^2$s .

## 4. Timing

The *AGILE* mission will benefit of a new space-qualified $\gamma$-ray detector based on silicon-strips devices rather than a gas/wire spark chamber. This technological improvement will allow a dramatic $\gamma$-ray dead-time reduction, from 100 msec (*EGRET* ) to 200 $\mu$sec (*AGILE* ). This fact will improve studies on sources which require accurate timing such as PSRs (in combination with the timing information provided by GPS) and GRBs. For the first time, it will be possible to search for sub-millisecond transient events in GRBs.

A detailed description of the *AGILE* timing perfomance and an estimate of the *AGILE*

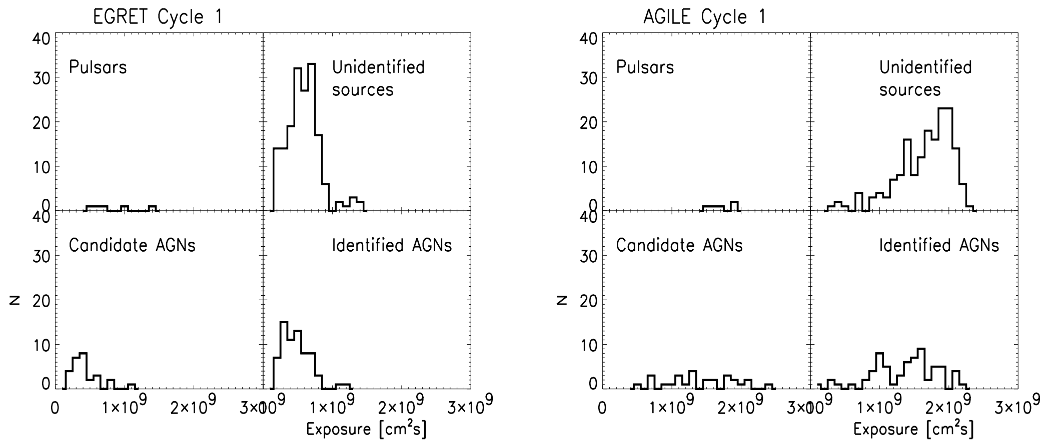


Fig. 6. *Left Panel: EGRET* Cycle-1 exposure distribution for different classes of gamma-ray sources. We considered the first year and half of *EGRET* observations (Apr. $22^{nd}$ 1991 - Nov. $17^{th}$ 1992). *Right Panel: AGILE* Cycle-1 exposure distribution for different classes of gamma-ray sources. We considered the first year of observation, simplifying the observation program into 6 major pointing directions, each divided into 10 sub-periods of approximately 1 week each.

detection capabilities of new $\gamma$-ray PSRs are given in Pellizzoni et al. (2004).

## 5. Conclusions and Summary

The wide FOV of *AGILE* will allow deep monitoring of $\gamma$-ray sources, improving variability studies and reducing the error box for source localization. At the completion of its Cycle-1, *AGILE* will have covered the entire sky, and the exposure accumulated on the unidentified sources will be, on average, 3 times that accumulated by *EGRET* during its 18-month Cycle-1, and thus comparable to the exposure accumulated by *EGRET* at the completion of its first four observing Cycles (due to the limited gas supply and efficiency).

The pointing strategy for the second *AGILE* observing Cycle could be more focused on particular sources. A possible observing plan could envision a 6-month scan of the Galactic Center, and a 3-month deep pointing towards the North and South Celestial Poles, which are the sky regions less occulted by the Earth and which can maximize the exposure throughput. This observing plan could be a complement to the all-sky scan survey that *GLAST* will perform, presumably, simultaneously with the *AGILE* Cycle-2.

## References

Chen A.: 2004, *These Proceedings*
Gregory P.C. et al.: 1979, *Astron. J.* **84**, 1030
Hartman R.C. et al.: 1999, *Astrophys. J. Suppl.* **123**, 79
Pellizzoni et al.: 2001, *AIPC* **587**, 759
Pellizzoni et al.: 2004, *These Proceedings*
Tavani M. et al.: 1996, *Astron. Astrophys. Suppl. Ser.* **120**, 243
Tavani M. et al.: 1999, *Mem. Soc. Astron. It.* **70**, 201
Tavani M. et al.: 2004, *These Proceedings*